Intracellular zinc activates KCNQ channels by reducing their dependence on phosphatidylinositol 4,5-bisphosphate

Haixia Gao[a,b], Aurélien Boillat[a], Dongyang Huang[b], Ce Liang[b], Chris Peers[c], and Nikita Gamper[a,b,1]

[a]Faculty of Biological Sciences, University of Leeds, Leeds LS2 9JT, United Kingdom; [b]Department of Pharmacology, Hebei Medical University, Shijiazhuang, China 050017; and [c]Leeds Institute of Cardiovascular and Metabolic Medicine, Faculty of Medicine and Health, University of Leeds, Leeds LS2 9JT, United Kingdom

M-type (Kv7, KCNQ) potassium channels are proteins that control the excitability of neurons and muscle cells. Many physiological and pathological mechanisms of excitation operate via the suppression of M channel activity or expression. Conversely, pharmacological augmentation of M channel activity is a recognized strategy for the treatment of hyperexcitability disorders such as pain and epilepsy. However, physiological mechanisms resulting in M channel potentiation are rare. Here we report that intracellular free zinc directly and reversibly augments the activity of recombinant and native M channels. This effect is mechanistically distinct from the known redox-dependent KCNQ channel potentiation. Interestingly, the effect of zinc cannot be attributed to a single histidine- or cysteine-containing zinc-binding site within KCNQ channels. Instead, zinc dramatically reduces KCNQ channel dependence on its obligatory physiological activator, phosphatidylinositol 4,5-bisphosphate (PIP$_2$). We hypothesize that zinc facilitates interactions of the lipid-facing interface of a KCNQ protein with the inner leaflet of the plasma membrane in a way similar to that promoted by PIP$_2$. Because zinc is increasingly recognized as a ubiquitous intracellular second messenger, this discovery might represent a hitherto unknown native pathway of M channel modulation and provide a fresh strategy for the design of M channel activators for therapeutic purposes.

M channel | KCNQ | Kv7 | zinc | phosphatidylinositol 4,5-bisphosphate

M-type (KCNQ, Kv7) K$^+$ channels are a family of voltage-gated K$^+$ channels with a very distinctive and robust role in the control of cellular excitability. The channels give rise to non-inactivating K$^+$ currents with slow kinetics and a very negative activation threshold (−60 mV or even more negative). In combination, these features allow KCNQ channels to remain partially active at voltages near the resting membrane potential of a neuron or a muscle cell and thus strongly influence excitability (1, 2). Transient KCNQ channel inhibition leads to reversible increases in neuronal excitability, whereas long-term losses of KCNQ channel activity often result in debilitating excitability disorders (1, 2). Thus, loss-of-function mutations within KCNQ genes underlie some types of epilepsy, deafness, and arrhythmias, whereas transcriptional down-regulation in sensory nerves may result in chronic pain (2). Conversely, M channel enhancers ("openers") reduce excitability and are clinically used as antiepileptic drugs (e.g., retigabine) or analgesics (e.g., flupirtine) (3). The therapeutic utility of KCNQ channel openers extends to other disorders linked to deregulated excitability, such as anxiety, stroke, and smooth muscle disorders (2, 3); therefore a global quest for specific and selective KCNQ openers is currently underway (3).

The KCNQ channel family contains five members, KCNQ1–5 (Kv7.1–Kv7.5). KCNQ1 is expressed mostly within the cardiovascular system, whereas the other members are predominantly neuronal (1, 2). The most abundant M-type channel within the nervous system is believed to be the heteromeric KCNQ2/3 channel, although other homo- and heteromeric channels are also present (1, 2).

In addition to voltage, KCNQ channels are also sensitive to the plasma membrane phosphoinositide phosphatidylinositol 4,5-bisphoshpate (PIP$_2$) (4, 5). Accordingly, G protein-coupled receptor-mediated PIP$_2$ depletion is one of the major mechanisms of the excitatory action of endogenous neurotransmitters and neuromodulators such as acetylcholine, angiotensin II, glutamate, and others (reviewed in refs. 1 and 2). Excised-patch single-channel recordings of KCNQ2–4 and KCNQ2/3 channels revealed that their open probability (P_o) approaches zero when PIP$_2$ is depleted, whereas increasing concentrations of exogenous PIP$_2$ raise the P_o up to unity (6). It also has been determined that KCNQ3 has a more than 20-fold higher apparent affinity for PIP$_2$ than KCNQ2 or KCNQ4 (6, 7). As a result, tonic membrane PIP$_2$ levels in cells such as CHOs are sufficient to maintain the P_o of KCNQ3 homomers at near unity (at saturating voltages), whereas homomeric KCNQ2 and KCNQ4 channels display very low P_o values of 0.1–0.2 (6, 8). The elucidation of the structural background of the interaction of the KCNQ channel with PIP$_2$ is ongoing, but several important regions have been identified, including two clusters of positively charged amino acid residues within the channel C terminus as well as additional clusters within the cytosolic S2–S3 and S4–S5 linkers (reviewed in ref. 9). All the regions identified thus far are cytosolic and are presumed to facilitate interactions with the negatively charged phosphate groups of PIP$_2$ facing the cytosol at the inner plasma membrane leaflet. Phosphorylation (10) or methylation (11) of residues within the C-terminal PIP$_2$-binding site were reported to modulate PIP$_2$ affinity and, in turn, KCNQ channel activity. Thus, modulation of

Significance

M-type (Kv7, KCNQ) potassium channels are powerful regulators of neuronal and muscular excitability and are validated drug targets for the treatment of excitability disorders. The plasma membrane phosphoinositide phosphatidylinositol 4,5-bisphosphate (PIP$_2$) is required to maintain M channel activity. We report that intracellular free zinc directly and reversibly augments the activity of recombinant and native M channels by reducing or virtually abolishing the channel requirement for PIP$_2$, thereby permitting a PIP$_2$-gated ion channel to operate independently of this important signaling molecule. Given the growing recognition of zinc as an intracellular second messenger, this phenomenon might represent a hitherto unknown pathway of M channel modulation and provide a fresh strategy for design of M channel-targeting drugs.

the KCNQ channel PIP_2 sensitivity may represent a therapeutic approach to the treatment of excitability disorders such as epilepsy and pain.

In the present study we report that intracellular zinc ions potently augment the activity of heterologous and native KCNQ channels by reducing channel requirements for PIP_2. The effect of zinc is reversible and most likely is direct, because it can be demonstrated in excised membrane patches. Because zinc is increasingly recognized as an important intracellular second messenger, this effect could represent an alternative regulatory signaling pathway for control over cellular excitability. Although intracellular concentrations of free zinc are low (<1 nM) (12), zinc is accumulated at high levels in various stores, such as the endoplasmic reticulum, mitochondria, and synaptic vesicles. In the synaptic vesicles, the concentrations of free zinc could reach the millimolar level (13). During synaptic transmission vesicular zinc is released, and quantities of zinc translocate to the postsynaptic terminals through zinc-permeable channels such as AMPA receptors (14). Additionally, zinc can be released from cytosolic buffering proteins such as metallothioneins, e.g., in response to acidification (15). Thus, there is clear scope for intracellular zinc signaling in neurons, including postsynaptic rises during periods of high activity, hypoxia, neurotrauma, and other conditions. Therefore, this acute and rapidly reversible mechanism for tuning KCNQ channel PIP_2 sensitivity by zinc might represent a neuronal feedback mechanism for controlling excitability during periods of hyperexcitability. However, because M channel potentiation requires micromolar levels of intracellular zinc, future research is needed to establish if native M channels are indeed subjected to such local concentrations of zinc under physiological or pathophysiological conditions in vivo.

Results

Zinc Ionophores Are KCNQ Channel Openers. Recent reports (16, 17) identified zinc pyrithione (ZnPy) (Fig. S1) as an atypical KCNQ channel opener and suggested that the pyrithione moiety (complexed with zinc) augments KCNQ channel activity by binding to a site within the extracellular pore region (16). It is also well recognized that ZnPy is a zinc ionophore that can effectively deliver free zinc ions across the plasma membrane of living cells (18, 19). Thus, we tested whether the effect of ZnPy on KCNQ channel activity is attributable to ZnPy's ionophore activity. To this end we overexpressed human KCNQ4 channels in CHO cells and tested the effect of five structurally distinct zinc ionophores on KCNQ4 currents. The following ionophores were used (Fig. S1): ZnPy (10 μM) (18), pyrrolidinedithiocarbamate (PDTC) (20 μM) (20), zinc diethyldithiocarbamate (Zn-DEDTC) (30 μM) (21), tetrabutylthiuram disulphide (zinc ionophore I) (20 μM) (22), and 5,7-Diiodo-8-hydroxyquinoline (DIQ) (50 μM) (23). ZnPy and Zn-DEDTC already contained zinc as part of the complex; other ionophores were used in combination with 25 μM $ZnCl_2$ in the extracellular solution. KCNQ4 was chosen because among homomeric Kv7 channels it displays the most reproducible and robust expression in CHO cells (24). Live confocal imaging of intracellular free zinc levels confirmed that all five ionophores produced robust elevations of intracellular zinc (Fig. 1 *A–F*); in each case these elevations were completely reversed by the application of the zinc chelator *N,N,N′,N′*, tetrakis (2-pyridylmethyl) etylenediaminepentaethylene (TPEN) (20 μM). TPEN has much higher zinc affinity than other ionophores such as ZnPy and DIQ ($K_d = 10^{-15.6}$ vs. $K_d \sim 10^{-5}$–10^{-8} M) (25, 26) and is capable of stripping zinc off intracellular proteins (25) and zinc-sensitive fluorescent indicators (19). We then performed perforated patch voltage-clamp recordings to test the effects of these five ionophores on KCNQ4 current amplitude. Strikingly, despite having different chemical structures, all five compounds augmented KCNQ4 amplitude by two- to threefold (Fig. 1 *G–L*). As were intracellular zinc levels, the effect of each ionophore on KCNQ4

current amplitude was reversed by TPEN. Notably, TPEN did not normally inhibit KCNQ4 current below the baseline but only reversed the ionophore-induced augmentation (Fig. 1*L*), suggesting that (*i*) the effect of TPEN is likely to be mediated by zinc chelation rather than by a direct effect on the channel, and (*ii*) tonic cytosolic levels of free zinc in CHO cells are too low to affect channel activity. Similar to KCNQ4, the heteromultimeric KCNQ2/3 channels formed by KCNQ2–KCNQ3 concatemers overexpressed in CHO cells were potently augmented by ZnPy, Zn-DEDTC, and PDTC; these effects were completely reversed by TPEN (Fig. 2 *A* and *B*). In accord with previous findings, ZnPy induced leftward shifts of the voltage dependence of KCNQ4 and KCNQ2/3 from −20.2 ± 1.8 mV to −39.8 ± 1.7 mV ($n = 8$; $P <$ 0.001) and from −23.2 ± 1.1 mV to −28.6 ± 2.0 mV ($n = 6$; $P =$ 0.089), respectively (Fig. S2).

Interestingly, Na^+ pyrithione (NaPy) (10 μM) also induced KCNQ4 current augmentation. The effect was slower and smaller in amplitude than that induced by ZnPy but nevertheless was significant (Fig. S3 *A* and *B*). Thus, NaPy augmented KCNQ4 current by 1.6 ± 0.1-fold ($n = 7$; $P < 0.01$) and subsequent transient application of ZnPy to the same cells caused further augmentation (2.1 ± 0.3-fold relative to baseline), which was significantly higher than the NaPy effect ($P < 0.01$) (Fig. S3 *A* and *B*). Finally, the application of TPEN (in the presence of NaPy) reverted the current amplitude to values that were slightly (but not significantly) below the baseline. Surprisingly, zinc imaging revealed that extracellular application of NaPy produced a moderate but significant elevation of intracellular zinc (Fig. S3*C*). We used atomic absorption spectroscopy to determine if our NaPy reagent (purchased from Sigma) was contaminated by zinc but found that the contamination was negligible. Thus, the 100 mM solution of NaPy contained 1.4 ± 0.5 μM zinc ($n = 4$), and in lower dilutions zinc was not reliably detectable. Therefore it is likely that the effect was a result of zinc release from intracellular stores; alternatively, it could be a result of a pyrithione-mediated zinc influx from the extracellular side, because extracellular solutions, although nominally zinc-free, do contain micromolar zinc traces (19). However, regardless of the source, it is clear that (*i*) NaPy produces increases in the intracellular free zinc concentration, and (*ii*) the augmentation of KCNQ4 current by NaPy is reversed by the zinc chelator TPEN. Thus, we conclude that the action of intracellular zinc is responsible for the augmentation of the KCNQ4 current by NaPy.

Intracellular Zinc Can Augment the Activity of Unitary KCNQ Channels. Experiments thus far established a correlation between the intracellular zinc levels and the amplitude of the macroscopic KCNQ current. To determine whether intracellular zinc alone is sufficient to augment KCNQ channel activity, we performed inside-out excised patch recordings of unitary KCNQ2/3 concatemeric channels overexpressed in CHO cells (as described in ref. 6; also see *Methods*). We measured single-channel P_o at a saturating voltage (0 mV). Patches with some single-channel activity in the cell-attached mode were excised into the inside-out configuration; upon excision, channel activity declined sharply, displaying almost no activity (Fig. 2 *C–F*), in accord with previous findings (6, 27). This sharp rundown of channel activity upon patch excision is likely caused by the depletion of membrane PIP_2 by the membrane-bound lipid phosphatases present in the patch membrane and is characteristic of virtually all PIP_2-sensitive ion channels (28). The addition of increasing concentrations of $ZnCl_2$ to the intracellular side of the patch produced concentration-dependent restoration of KCNQ2/3 channel activity so that the P_o rose from nearly zero to 0.26 ± 0.09, 0.68 ± 0.07, and 0.75 ± 0.05 at 10, 50, and 100 μM $ZnCl_2$, respectively ($P < 0.001$; $n = 5$) (Fig. 2 *C–F*). In our experiments the amplitudes of single concatemeric KCNQ2/3 channel currents at 0 mV were somewhat higher than those reported for channels formed by independently overexpressed KCNQ2 and
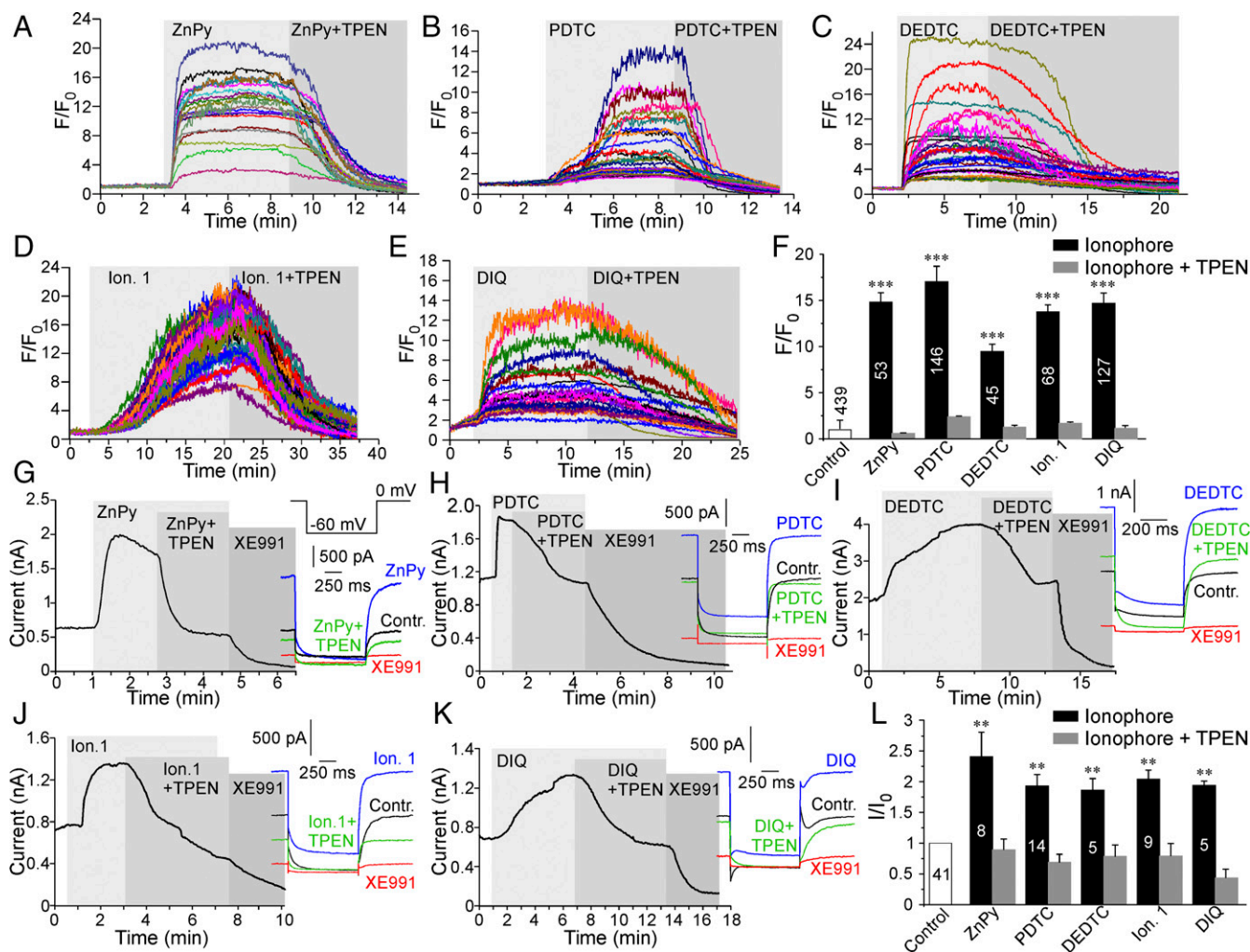
Fig. 1. Zinc ionophores potentiate KCNQ4. (*A*–*E*) Fluorescence imaging of CHO cells loaded with the zinc fluorophore FluoZin-3 AM. Shown are examples of changes in the time course of FluoZin-3 fluorescence during application of ZnPy (10 μM) (*A*), PDTC (20 μM) (*B*), Zn-DEDTC (30 μM) (*C*), zinc ionophore I (20 μM) (*D*), and DIQ (50 μM) (*E*). PDTC, DIQ, and zinc ionophore I were supplemented with 25 μM $ZnCl_2$. At the end of each recording the zinc chelator TPEN (20 μM) was added (still in the presence of the appropriate ionophore). In these and all other time-course plots, periods of drug applications are indicated by gray shading. (*F*) Summary of the experiments presented in *A*–*E*. (*G*–*K*) Perforated patch-clamp recordings from KCNQ4-transfected CHO cells showing the time courses for the effects of zinc ionophores and TPEN (as labeled; applied as in *A*–*E*) on the amplitude of the KCNQ4 current. At the end of each recording a specific KCNQ channel inhibitor, XE991 (10 μM), was applied. Examples of current traces are shown on the right; the voltage protocol is given in the *Inset* in *G*. (*L*) Summary of the experiments presented in *G*–*K*. In *F* and *L* the number of cells is indicated within the bars; asterisks indicate a significant difference from the basal fluorescence; **$P < 0.01$ and ***$P < 0.001$ (paired *t* test).

KCNQ3 subunits (1.21 ± 0.11 pA, $n = 7$ vs. ∼0.7 pA) (6, 7), although the kinetics and voltage dependence of the macroscopic currents were similar (Fig. S2 *C*–*D*). The single-channel experiments demonstrated that intracellular zinc ions are sufficient to augment KCNQ channel activity and thus most likely account for the KCNQ opener action of zinc ionophores. The application of $ZnCl_2$ (up to 50 μM) to the extracellular side of the plasma membrane in whole-cell experiments failed to augment KCNQ4 current but produced a weak inhibitory effect instead (Fig. S4).

Zinc Potentiates Native M Channels in Dorsal Root Ganglion Neurons. We next tested if zinc can potentiate the activity of native M channels. M channels are expressed in mammalian somatosensory neurons (especially in pain or nociceptive neurons) and are important for the control of their resting excitability (29, 30), ultimately controlling nociceptive signaling (reviewed in ref. 31). Thus, we tested the effect of intracellular zinc on the M current in cultured small-diameter (presumed nociceptive) rat dorsal root ganglion (DRG) neurons. Similar to the currents produced

by overexpressed KCNQ channels, the native M current in DRG neurons was also augmented by ZnPy (10 μM) to 1.65 ± 0.24 of the basal amplitude ($P < 0.01$; $n = 5$) (Fig. 3 *A* and *B*). This effect was completely reversed by 20 μM TPEN, which, however, did not inhibit the current significantly below the basal level. As in CHO cells, ZnPy also produced robust rises in intracellular zinc in cultured neurons (Fig. 3 *C* and *D*), an effect that again was reversed by TPEN.

To test if intracellular free zinc is sufficient for native M current augmentation, we performed whole-cell recordings with pipette solution supplemented with 50 μM $ZnCl_2$. In these recordings Ca^{2+}, Mg^{2+}, and Ca^{2+} buffers were excluded from the pipette solution. When the whole-cell configuration of the patch-clamp recording was broken into using the control pipette solution, there was a small run-up of M current amplitude (measured as tail current relaxation upon voltage pulse from −30 to −60 mV) (*Methods* and Fig. 3*E*). This run-up was significantly potentiated when recording with the pipette solution containing $ZnCl_2$. Accordingly, the plateau M current density was significantly larger in the $ZnCl_2$ solution
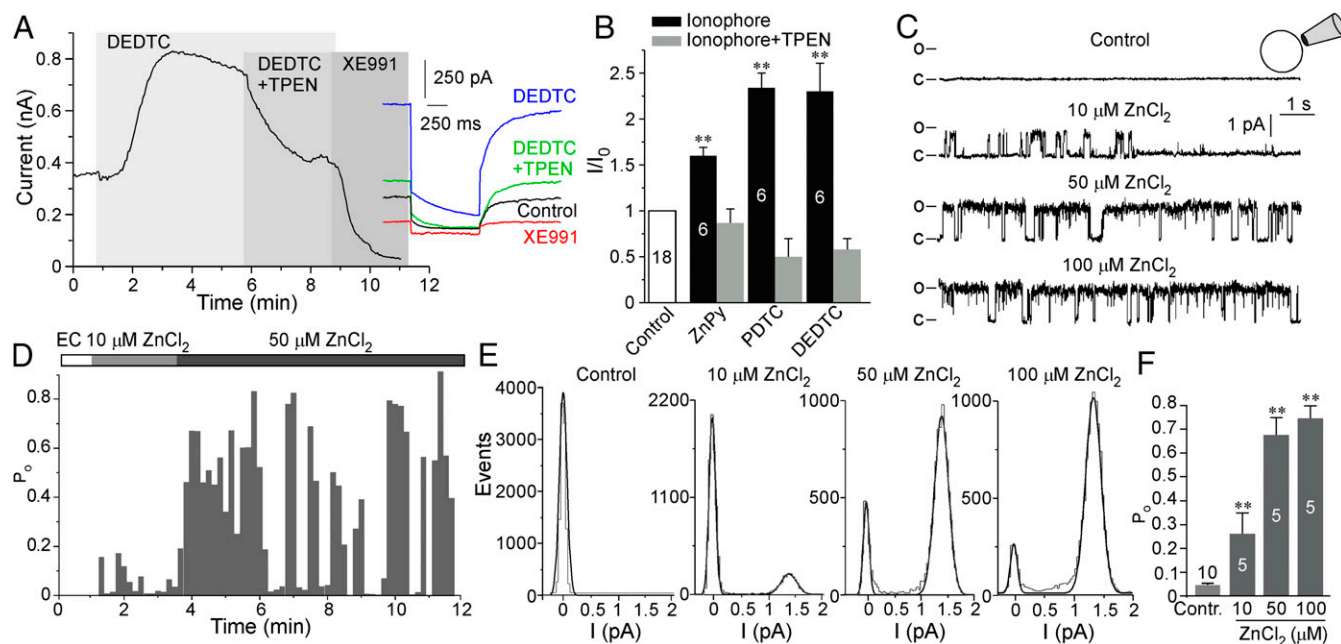
Fig. 2. Effect of intracellular zinc on KCNQ2/3 channels. (*A*, *Left*) Perforated patch-clamp recordings from CHO cells transfected with the KCNQ2/3 concatemer showing the effects of DEDTC (30 μM), TPEN (20 μM), and XE991 (10 μM) (as labeled) on the amplitude of the M current. (*Right*) Examples of current traces. (*B*) Summary of the effects of ZnPy, PDTC, and DEDTC on KCNQ2/3 currents; recordings were made as in *A* and in Fig. 1 *G–K*. (*C*) Current records from a patch of CHO cell membrane containing a single KCNQ2/3 channel in inside-out mode with various concentrations of $ZnCl_2$ in the cytoplasmically facing bath solution. (*D*) Each 10-s sweep during the experiment was analyzed for channel P_o, and the time course of the P_o during the experiment was plotted. (*E*) All-point amplitude histograms for the sweeps shown in *C*. (*F*) Summary of the effect of intracellular $ZnCl_2$ (10–100 μM) on the KCNQ2/3 P_o. In *B* and *F* the number of recordings is indicated within the bars; asterisks indicate a significant difference from the control; **$P < 0.01$ (paired *t* test).

than in the control condition (4.8 ± 0.3 pA/pF, $n = 14$ vs. 8.9 ± 1.0 pA/pF, $n = 14$; $P \leq 0.001$) (Fig. 3*F*). Thus, the native M current in DRG neurons is also potently augmented by intracellular zinc.

Modulation of the KCNQ Current by Zinc Is Mechanistically Distinct from the Redox-Dependent Augmentation of the KCNQ Current. Recently we and others reported augmentation of KCNQ channel activity via the oxidative modification of a triple-cysteine pocket in the channel S2–S3 linker (11, 24, 32). Because zinc can bind to cysteines and form redox-sensitive molecular switches (33), we tested if the effect of zinc on KCNQ channels is also redox dependent and mediated by the triple-cysteine pocket. We compared the effect of zinc with that of ascorbate, the latter having been shown to augment KCNQ4 channel activity in a redox-dependent way (32). In accord with previous findings, application of 2 mM ascorbate caused a 2.5 ± 0.9-fold increase in the amplitude of the KCNQ4 current ($P \leq 0.01$; $n = 6$) (Fig. 4 *A*, *B*, and *G*); this effect was reversed by the reducing agent DTT (2 mM) (Fig. 4 *A* and *G*). In contrast, TPEN (20 μM) did not reverse the ascorbate-induced augmentation of the KCNQ4 current (Fig. 4 *B* and *G*). Zinc imaging revealed that ascorbate does not produce a measurable increase in intracellular zinc (Fig. S5). On the other hand, the KCNQ4-potentiating effect of ZnPy (and other zinc ionophores) was reversed by TPEN (Figs. 1 *G–L* and 4 *D* and *H*) but not by DTT (Fig. 4 *C* and *H*). Most importantly, substitution of three cysteines within the redox-sensitive cysteine pocket by alanines [C(156–158)A] in KCNQ4 resulted in a channel that was completely insensitive to ascorbate (Fig. 4 *E* and *I*), but the C(156–158)A mutant channel currents were still sensitive to ZnPy (3.1 ± 0.7-fold potentiation, $n = 5$; not different from WT KCNQ4) (Fig. 4 *F* and *I*). These experiments suggest that the augmentation of KCNQ currents by zinc is mechanistically distinct from the effect produced by oxidative modification within the reactive cysteine pocket.

In Search of the KCNQ Zinc-Binding Site. Zinc binding sites in proteins usually contain histidine or cysteine residues (with aspartic or glutamic acids also often participating in zinc coordination) (34). To identify a zinc-binding site within the KCNQ channels, we substituted with alanines all of the individual intracellular histidines and also the intracellular cysteines conserved between KCNQ2–4 (Fig. 5*A*, *Inset*); we used KCNQ4 as a backbone for these experiments. These substitutions included the following residues: histidines at the positions 102, 234, 330, 334, 569, and 669 and cysteines at the positions 112, 156–158, 175, 418, 427, and 519. We also tested a KCNQ4 channel with a histidine-less C terminus, H(330,334,569,669)A, and a triple-cysteine substitution at positions C(156–158)A (see above). Surprisingly, none of these individual or group histidine or cysteine substitutions abolished channel sensitivity to ZnPy (Fig. 5*A*). Only in the H569A mutant was the current augmentation somewhat lower (1.6 ± 0.2-fold increase, $n = 7$ vs. 2.4 ± 0.4-fold in WT KCNQ4, $n = 8$), but this difference was not statistically significant. These experiments revealed that neither intracellular histidines nor cysteines (either individually or in clusters) can fully account for zinc-induced KCNQ current potentiation, and thus some other mechanisms must be involved.

Surprisingly, H334A displayed dramatically enhanced ZnPy-induced potentiation compared with WT KCNQ4 (Fig. 5*A* and Fig. S6); the mutant also had much smaller basal current amplitude (Fig. S6 *B* and *D*). A similar tendency (although less pronounced) was displayed by the quadruple-His mutant, which also has H334 replaced (Fig. 5*A* and Fig. S6 *C* and *D*). Interestingly, H334 in KCNQ4 is equivalent to H328 in KCNQ2, a residue that was identified as one of the key determinants of channel interaction with PIP_2 (5). The reduced apparent affinity to PIP_2 of H334A mutant correlates well with reduced baseline current amplitude. However, the strong enhancement of the baseline current by ZnPy to levels even higher than those produced by WT KCNQ4 may suggest that zinc reduces the channel
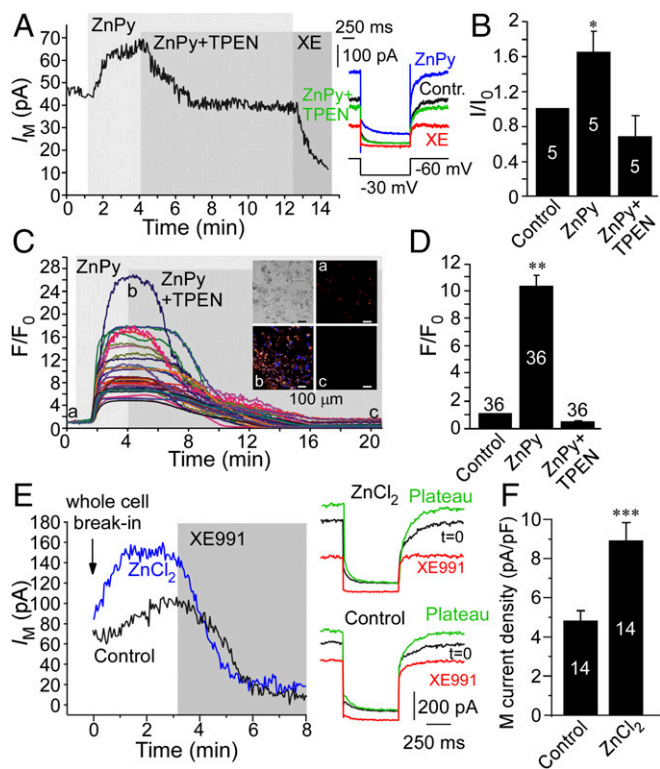
Fig. 3. Effect of intracellular zinc on the endogenous M current in DRG neurons. (*A*, *Left*) Time course of the effect of ZnPy (10 μM), TPEN (20 μM), and XE991 (3 μM) on the M-like K$^+$ current (I_M) recorded from the small-diameter cultured rat DRG neuron. (*Right*) Examples of current traces are shown, and the voltage protocol is depicted below the traces. (*B*) Summary of data in *A* (normalized current, I/I_0). (*C*) Fluorescence imaging of DRG cultures loaded with the zinc fluorophore FluoZin-3 AM. Shown is an example of the time course of changes in FluoZin-3 fluorescence during the application of ZnPy (10 μM) and TPEN (20 μM). (*Inset*) Examples of fluorescence micrographs. F/F$_o$, fluorescence intensity relative to baseline. (*D*) Summary of data in *C*. (*E*) Examples of time courses of changes in the amplitude of the M-like current in DRG neurons when the whole-cell configuration is broken with a pipette solution containing no added zinc, Ca^{2+}, or divalent cation buffers (Control) or with the same solution supplemented with 50 μM ZnCl$_2$. (*F*) Summary of the data in *E*. In *B*, *D*, and *F* the number of recordings is indicated within the bars. Asterisks indicate a significant difference from the control; *$P < 0.05$, **$P < 0.01$ or ***$P < 0.001$ (paired or unpaired t test).

requirements for PIP$_2$. Our single-channel experiments also suggested the same hypothesis: KCNQ channels have a permissive requirement for PIP$_2$, and when membrane PIP$_2$ is depleted, as in an inside-out excised patch (28), the activity in single KCNQ channels runs down rapidly to almost zero (Fig. 2 *C–F*) (5, 6). However, the addition of zinc to the intracellular side of the plasma membrane was able to rescue the KCNQ channel activity without replenishment of PIP$_2$. We therefore asked if zinc can indeed interfere with the channel requirement for PIP$_2$.

Zinc Reduces the Dependence of the KCNQ Channel on PIP$_2$. First, we tested the effect of intracellular zinc on KCNQ3, a channel that, in contrast to KCNQ2 and KCNQ4, has high PIP$_2$ affinity (6), so that tonic PIP$_2$ levels in CHO cells are sufficient to maintain the tonic maximal P_o of this channel near unity (6). Because the KCNQ3 channel expresses poorly as a homomer (35, 36), we used KCNQ3 with a pore domain mutation, A315T (KCNQ3^T), which strongly increases the amplitude of the KCNQ3 current without changing apparent PIP$_2$ affinity (7, 36, 37). Interestingly, neither ZnPy nor PDTC had any effect on the amplitude of the

KCNQ3^T current (Fig. 5 *B*, *D*, *E*, and *G*), suggesting that the effects of PIP$_2$ and zinc on channel activity are nonadditive; thus zinc would have little effect on a given KCNQ subunit when the level of PIP$_2$ is saturating.

We then disabled two known C-terminal PIP$_2$-interacting sites in KCNQ3^T by (*i*) deleting a linker between helices A and B (positons 411–508) that harbors a cluster of basic residues (including K425, K432, and R434) (38) and (*ii*) introducing the mutations R364A and H367C that neutralized the PIP$_2$-interacting site at the junction between S6 and C-terminal helix A (5, 39); we labeled this mutant "KCNQ3^T-ΔPIP$_2$-C$_{term}$." Charge-neutralizing mutations within either of these sites were shown to reduce channel PIP$_2$ affinity (5, 38, 39). Accordingly, the amplitude of the KCNQ3^T-ΔPIP$_2$-C$_{term}$
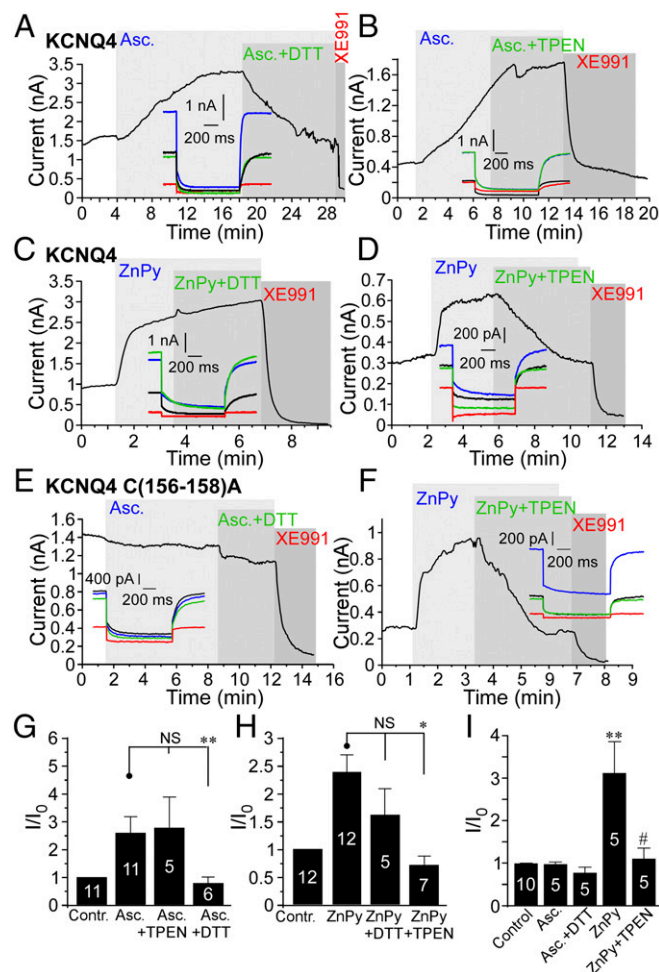
Fig. 4. The mechanism of KCNQ channel potentiation by zinc is distinct from the redox-dependent modulation. (*A* and *B*) Perforated patch-clamp recordings from KCNQ4-transfected CHO cells. The augmentation of KCNQ4 current by ascorbate (Asc.) (2 mM) was reversed by the reducing agent DTT (2 mM) (*A*) but not by 20 μM TPEN (*B*). Examples of current traces are shown in the *Insets*. (*C* and *D*) As in *A* and *B* but with ZnPy (10 μM) applied instead of ascorbate. In this case the KCNQ4 augmentation was reversed by TPEN but not by DTT. (*E* and *F*) The effect of ascorbate (*E*) but not of ZnPy (*F*) is abolished in KCNQ4 channels with C-to-A substitutions at positions 156, 157, and 158. (*G–I*) Summaries of the ascorbate (*G*) and ZnPy (*H*) experiments on WT KCNQ4 and the experiments on the KCNQ4 C(156–158)A (*I*). The number of recordings is indicated within the bars. Asterisks in *G* and *H* denote a significant difference from the group indicated by the line connector; *$P < 0.05$ and **$P < 0.01$ (paired t test). Symbols in *I* indicate a significant difference from control (**$P < 0.001$; paired t test) or from current amplitude in the presence of ZnPy (#$P < 0.05$; paired t test).

Gao et al.
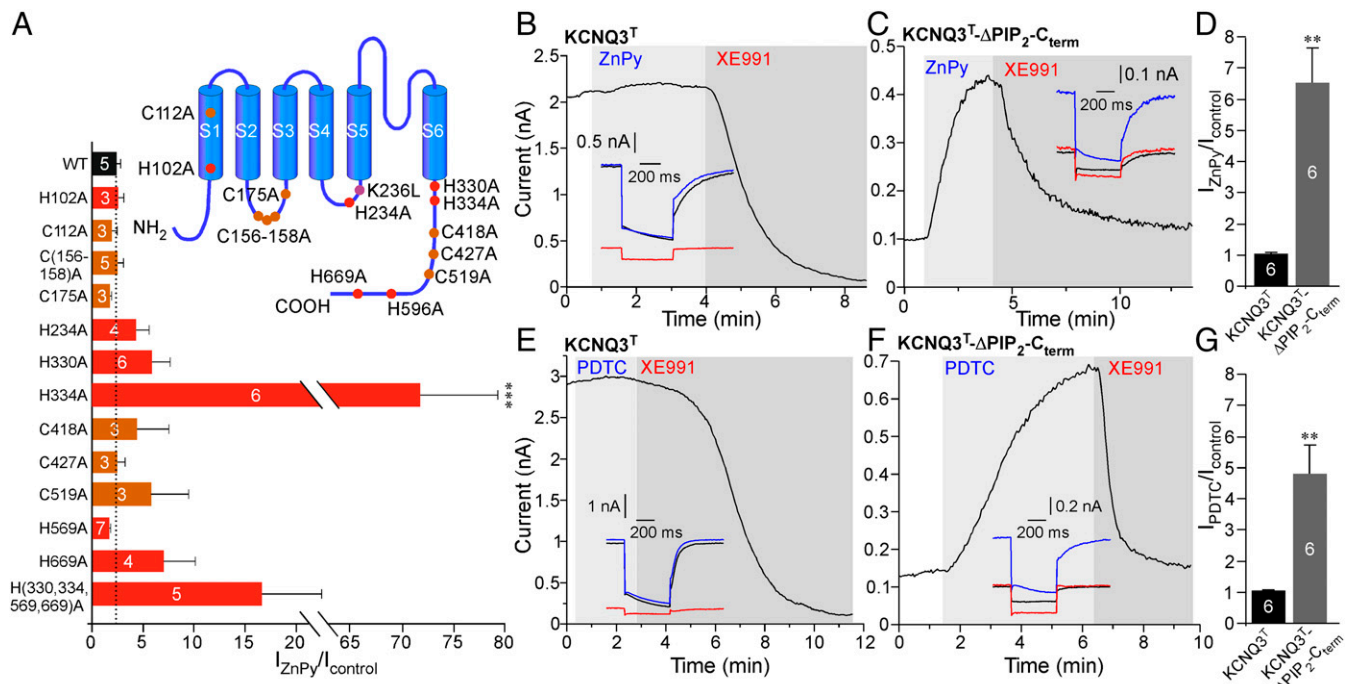
Fig. 5. Intracellular zinc affects KCNQ channel interaction with PIP$_2$. (*A*) Summary of the ZnPy-induced current augmentation (normalized to baseline) for single C-to-A and H-to-A KCNQ4 mutants and for the C(156–158)A triple mutant and the H(330,334,569,669)A quadruple mutant expressed in CHO cells. A schematic depiction of substitutions is shown in the *Inset*. Asterisks indicate significant difference from WT KCNQ4; ***$P < 0.001$ (one-way ANOVA with Bonferroni correction). (*B–G*) Comparison of the effects of 10 μM ZnPy (*B–D*) and 20 μM PDTC (*E–G*) on the amplitude of the KCNQ3 A315T (KCNQ3^T; *B* and *E*) or KCNQ3^T with the C-terminal PIP$_2$-interacting sites neutralized: deletion of the A–B linker (positons 411–508) and R364A and H367C substitutions (KCNQ3^T-ΔPIP$_2$-C$_{term}$; *C* and *F*). Effects are summarized in *D* and *G*. The number of experiments is indicated within the bars. Asterisks indicate a significant difference from control (**$P < 0.001$; paired *t* test).

current was reduced more than 10-fold compared with the KCNQ3^T channel (103.25 ± 28.34 pA, $n = 12$ vs. 1,170 ± 370 pA, $n = 10$, $P \leq 0.001$). Strikingly, both ZnPy and PDTC produced five- to sevenfold augmentation of the KCNQ3^T-ΔPIP$_2$-C$_{term}$ current amplitude (Fig. 5 *C*, *D*, *F*, and *G*). These data suggest that the increased PIP$_2$ dependence of the KCNQ3^T-ΔPIP$_2$-C$_{term}$ mutant can be compensated by intracellular zinc.

Next, we used a similar strategy to reduce the affinity of KCNQ4 for PIP$_2$ to test how this change would affect the effects of zinc on this channel. This time we targeted a different PIP$_2$-interacting site, the S4–S5 linker. We neutralized one of the basic residues by introducing a K236L substitution (Fig. 5*A*, *Inset*) at a position equivalent to K222 in KCNQ3, which was shown to be involved in the interaction with PIP$_2$ (17). As with KCNQ3^T-ΔPIP$_2$-C$_{term}$, the current amplitude of the KCNQ4 K236L mutant was much lower than that of WT KCNQ4 (Fig. S7 *A–D*). However, ZnPy produced much stronger current augmentation of the mutant: 16.1 ± 4.4-fold ($n = 10$) vs. 2.4 ± 0.4-fold ($n = 7$; $P \leq 0.01$) (Fig. S7 *A*, *B*, and *E*). To probe further the relationships between the channel PIP$_2$ requirement, PIP$_2$ levels, and potentiation by zinc, we increased tonic PIP$_2$ levels in CHO cells by overexpressing the key enzyme of PIP$_2$ synthesis, PI(4)5-kinase (which phosphorylates phosphatidylinositol 4-phosphate to PIP$_2$); this maneuver has been shown to increase maximal P_o and the macroscopic current density of KCNQ2 and KCNQ2/3 in CHO cells (6). PI(4)5-kinase overexpression indeed significantly increased current amplitudes of both WT KCNQ4 and KCNQ4 K236L and, as expected, had a stronger effect on the latter (Fig. S7 *C* and *D*). In CHO cells overexpressing PI(4)5-kinase, ZnPy still augmented current amplitudes of both WT and K236L mutant channels, but, notably, the maximal current amplitudes in the presence of ZnPy were the same in CHO cells with and without PI(4)5-kinase overexpression (Fig. S7 *C* and *D*). Accordingly, the degree of the ZnPy-induced

augmentation of the KCNQ4 K236L current (relative to baseline) in the presence PI(4)5-kinase was strongly reduced (Fig. S7*E*) and was no longer different from the augmentation of WT KCNQ4 in the absence of PI(4)5-kinase.

Collectively, the experiments presented in Fig. 5 *B–G* and Fig. S7, together with the single-channel data (Fig. 2 *C–F*), suggest that (*i*) at saturating PIP$_2$ levels intracellular zinc can no longer increase channel activity; (*ii*) the lower the level of channel saturation with PIP$_2$, the higher is the augmenting effect of zinc; and (*iii*) even when PIP$_2$ saturation is below the threshold for channel activation (e.g., in inside-out patches), KCNQ channels can still be activated by zinc.

Finally, we asked how the presence of intracellular zinc affects the sensitivity of the KCNQ channel to acute PIP$_2$ depletion and recovery. We used the voltage-sensitive phosphatase from *Ciona intestinalis* (ciVSP). This enzyme is activated by strong depolarization; when overexpressed, it is capable of robustly depleting membrane PIP$_2$ (40) and almost completely inhibiting KCNQ channel activity (41, 42). We overexpressed ciVSP with either KCNQ4 or with KCNQ2/3 concatemer in CHO cells and recorded currents during the ciVSP activation. Cells were held at −80 mV, and three-step pulses (Fig. 6*A$_1$*) were applied: (*i*) a 1-s step to −20 mV [close to the threshold for ciVSP activation (40, 43) but near the half-maximal voltage for KCNQ channel activation (2)]; (*ii*) a 1-s step from −20 mV to 120 mV [close to the saturating voltage for ciVSP (40, 43)]; and (*iii*) a 30-s step from 120 mV to −20 mV. At the end of the protocol voltage was returned to the holding potential. In the control conditions during step *i*, KCNQ channels are activated; during step *ii* the KCNQ channel current is first increased because of the increased driving force but then begins to decline because of the ciVSP activation and PIP$_2$ depletion. At the beginning of step *iii* PIP$_2$ is depleted, and KCNQ channels are inhibited, but because of the ciVSP

Fig. 6. Intracellular zinc abolishes KCNQ channel inhibition by the voltage-sensitive phosphatase ciVSP. (*A* and *B*) Effects of 10 μM ZnPy (*A*) and 20 μM PDTC (*B*) on the ciVSP-induced inhibition of KCNQ2/3 concatemers in CHO cells. Examples of current traces are shown in A_1 and B_1; the voltage protocol is given in the *Inset* above traces in A_1. A_2 shows a time course of the effects of ZnPy and recovery by TPEN on the ciVSP-induced inhibition of KCNQ2/3 (the experiment shown in A_1). A_3 and B_2 summarize the effect of zinc ionophores on the ciVSP-induced KCNQ2/3 current inhibition. A_4 and B_3 summarize the recovery from the ciVSP-induced inhibition in control conditions and in the presence of the ionophore. The number of experiments is indicated within the bars. Symbols indicate a significant difference from control (***$P < 0.001$) and from ZnPy (###$P < 0.001$), respectively (paired *t* test). (*C* and *D*) As in *A* and *B*, but KCNQ4 was tested. NS, not significant. *E* shows confocal imaging of the effect of ciVSP activation by depolarization (150 mM extracellular KCl with or without 10 μM ZnPy, as indicated) on the membrane localization of the optical PIP$_2$ reporter PLC-δPH-GFP. An example of a time course is shown in E_1. Images taken at the times indicated by the letters in E_1 are shown in E_2; corresponding intensity line-scans (at the position indicated by the dotted red line in E_2, *a*) are shown below the images. The changes in cytosolic fluorescence intensity are summarized in E_3; the number of cells is indicated within the bars. Asterisks indicate significant difference from control; ***$P < 0.001$ (repeated measures ANOVA).

deactivation and PIP$_2$ resynthesis KCNQ activity recovers at the end of this step (black traces in Fig. 6 A_1, B_1, C_1, and D_1). Because steps *i* and *iii* are recorded at the same voltage (−20 mV), the difference between current amplitudes at the end of step *i* and the beginning of step *iii* represents the inhibition of the KCNQ current by the ciVSP-induced depletion of PIP$_2$, whereas the difference between the amplitudes at the end of step *i* and the end of step *iii* represents current recovery caused by PIP$_2$ resynthesis (41). In accord with previous findings, ciVSP activation induced 70–80% inhibition of both KCNQ2/3 (Fig. 6 *A* and *B*) and KCNQ4 (Fig. 6 *C* and *D*), and in both cases current completely recovered at the end of step *iii*. Application of either ZnPy or PDTC completely abolished PIP$_2$-dependent inhibition of both KCNQ channels (red traces in Fig. 6 A_1, B_1, C_1, and D_1). Application of TPEN after (and in the presence of) ZnPy,

restored the ability of ciVSP to inhibit the KCNQ2/3 channel (Fig. 6 A_1 and A_2).

To test if zinc inhibits ciVSP itself, we used an optical method of measuring ciVSP activity in which we coexpressed the enzyme in CHO cells together with KCNQ4 and the optical PIP$_2$ reporter PLC-δPH-GFP (44) and measured its translocation from membrane to cytosol in response to depolarization by an extracellular solution containing 150 mM KCl instead of NaCl (45). The intracellular K$^+$ concentration in CHO cells is ~140 mM (46); thus such a maneuver depolarized the membrane potential to approximately +2 mV, which is sufficient to trigger measurable ciVSP activation (43, 45). Accordingly, confocal imaging of the plasma membrane PIP$_2$ labeled by PLC-δPH-GFP revealed clear and reversible depolarization-induced PIP$_2$ depletion manifested in PLC-δPH-GFP translocation and an increase in cytosolic fluorescence
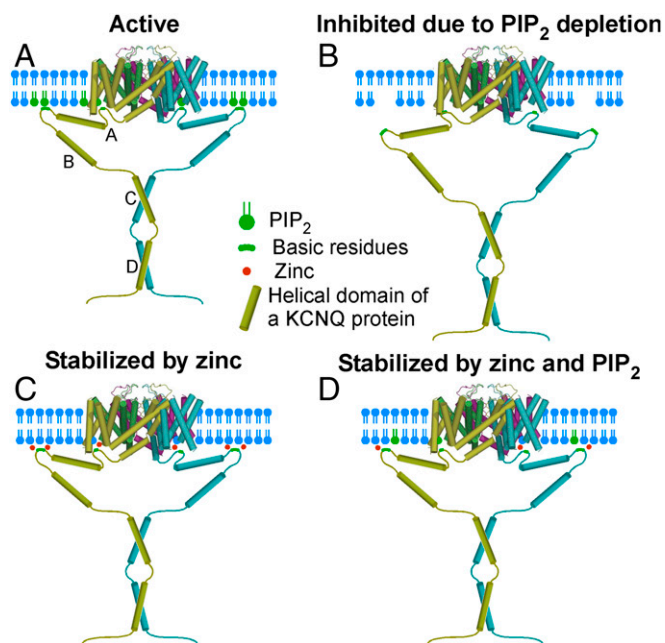
Gao et al.

Fig. 7. Hypothesis for the stabilization of the KCNQ channel by PIP$_2$ and intracellular zinc. (*A*) An active channel in the presence of a saturating PIP$_2$ concentration. (*B*) A channel inhibited by PIP$_2$ depletion (e.g., because of PLC or ciVSP activation). (*C*) A channel in the absence of membrane PIP$_2$ but stabilized by zinc, e.g., via shielding the negatively charged residues and coordinating the channel–membrane interface to strengthen the interactions with other phospholipids. (*D*) A scenario of a subsaturating membrane PIP$_2$ level when the channel activity is maximized by zinc because of the increased stability of the interaction with PIP$_2$ and other membrane phospholipids.

(and concomitant decrease in membrane fluorescence) (Fig. 6*E*). This translocation was not affected by the extracellular application of ZnPy, suggesting that zinc does not significantly affect ciVSP activity.

Muscarinic inhibition of KCNQ channels is mediated by G$_{q/11}$-induced activation of phospholipase C (PLC) via depletion of PIP$_2$ (4, 5). Additionally, inositol trisphosphate-dependent Ca^{2+} transients (mediated by calmodulin) and diacylglycerol-dependent PKC phosphorylation are also thought to contribute to muscarinic KCNQ channel inhibition. Both of these additional mechanisms are thought to work by decreasing channel PIP$_2$ affinity (reviewed in ref. 2). Thus, if intracellular zinc reduces channel dependence on PIP$_2$, muscarinic inhibition of KCNQ channels would be expected to be reduced or abolished in the presence of zinc. Indeed, in CHO cells overexpressing KCNQ4 and the M1 muscarinic receptor, the preapplication of ZnPy reduced the inhibition of KCNQ current by the M1-specific agonist oxotremorine-M (Oxo-M) from $69 \pm 9\%$ ($n = 7$) to $9 \pm 3\%$ ($n = 7$; $P < 0.01$) (Fig. S8).

Discussion

The major findings of this study are the following: (*i*) Intracellular zinc strongly potentiates native and recombinant KCNQ channel activity; (*ii*) any zinc ionophore is a potential KCNQ channel opener; (*iii*) zinc reversibly reduces or perhaps even abolishes the requirement of the KCNQ channel for PIP$_2$; and (*iv*) mechanistically, the zinc effect is distinct from the known redox-dependent KCNQ channel potentiation; also, the effect cannot be attributed to a histidine- or cysteine-containing binding site.

Several lines of evidence indicate that zinc strongly reduces the requirement of the KCNQ channel for PIP$_2$. Thus, (*i*) unitary KCNQ2/3 channel activity quickly runs down upon patch excision as a result of PIP$_2$ depletion (5, 28); however, the addition of free zinc to the intracellular side of the membrane maximizes

channel activity (Fig. 2 *C–F*). (*ii*) KCNQ3 is insensitive to zinc ionophores (Fig. 5 *B–G*) (17); this channel has highest apparent affinity for PIP$_2$ in the KCNQ family, and its tonic P_o max at saturating voltages is close to unity, presumably because of saturation with PIP$_2$ (6). Removal of C-terminal PIP$_2$-interacting residues resulted in a channel with much lower tonic activity, which can be rescued by intracellular zinc (Fig. 5 *B–G*). (*iii*) Similarly, the efficacy of ZnPy in augmenting KCNQ4 current is higher for the mutant with reduced PIP$_2$ affinity. (*iv*) Elevation of tonic PIP$_2$ levels by overexpression of PI(4)5-kinase reduced KCNQ channel sensitivity to zinc. (*v*) Finally, acute PIP$_2$ depletion by ciVSP or M1 receptor activation sharply inhibits KCNQ2/3 and KCNQ4 currents, but this inhibition is abolished by zinc (Fig. 6 *A–D* and Fig. S8). It appears that zinc can compensate for the channel's desaturation with PIP$_2$ because of either acute PIP$_2$ depletion or reduction in PIP$_2$ affinity. On the other hand, the more a channel protein is saturated with PIP$_2$, the lower is the zinc efficacy.

How might zinc interact with KCNQ channels and so dramatically affect channel–PIP$_2$ interaction, and is there a unique zinc-binding site? It is worth noting that interaction between KCNQ channels and PIP$_2$ cannot be pinpointed to a unique, localized binding site. Instead, the channel appears to form a broad PIP$_2$-interacting interface whereby basic residues, spread along all the main cytosolic domains of a channel, participate in electrostatic interactions with the negatively charged headgroup phosphates of PIP$_2$. Thus, basic residues in the S2–S3 linker (47, 48), the S4–S5 linker (17, 49), the S6-proximal C-terminal linker (5, 39), the C-terminal A–B helix linker (38), and the distal C terminus (49) were identified. Charge-neutralization mutations within most of these sites resulted in reduced apparent PIP$_2$ affinity and reduced tonic channel activity (reviewed in ref. 9). Another important point is that not only PIP$_2$ but also other phosphoinositides, such as PIP, PI(3,4)P, and PI(3,4,5)P (6, 27), and even other phospholipids, such as lysophosphatidic acid and sphingosine-1-phosphate (27), can activate KCNQ channels. Under normal physiological circumstances these interactions are thought not to affect KCNQ channel activity significantly because of the low plasma membrane abundance of these other lipids relative to that of PIP$_2$ (2, 27). However, should the affinity of channel–lipid interaction increase, these minor phospholipids may come into play. Therefore one explanation for the activating effect of zinc could be that it serves as electrostatic "glue" that stabilizes the interaction of the KCNQ channel's phospholipid interface with the inner leaflet of the plasma membrane (Fig. 7). Perhaps, by interacting with the negatively charged amino acid residues within the channel–membrane interface, zinc ions strengthen the interactions of the positively charged amino acids with negatively charged headgroups of phospholipids thus stabilizing channel opening. This effect may reduce the channel's selectivity toward phospholipids (so that other negatively charged lipids may become capable of substituting for PIP$_2$ anchoring) or dramatically increase its apparent affinity for PIP$_2$; a combination of both effects is also a possibility.

Interestingly, magnesium has been shown to decrease KCNQ channel activity, presumably by shielding PIP$_2$ and weakening the KCNQ channel–PIP$_2$ interaction (50). It is unclear why zinc and magnesium have such different effects on KCNQ channel activity; however, one consideration is that as a transition metal, zinc has a much higher ability than magnesium to form chelate complexes (see e.g., www.coldcure.com/html/stability_constants.html) and, potentially, to coordinate tertiary protein structures. Thus, zinc might be better suited to stabilize KCNQ channel–membrane interactions. However, future structural studies are required to address this question comprehensively.

Another intriguing question is whether the PIP$_2$-rescue effect of zinc can affect other PIP$_2$-sensitive channels. We tested the effect of ZnPy on another PIP$_2$-sensitive channel, Kir2.3 (51), and on a

PIP$_2$-insensitive channel, Kv1.4 (42). Both of these channels were inhibited by ZnPy to a differing degree ([Fig. S9]). The likely explanation here is that zinc might act as a pore blocker or inhibitor of these channels; there could also be additional inhibitory mechanisms (e.g., induced by the ionophore). Thus, although zinc may indeed reduce the PIP$_2$ dependence of other PIP$_2$-sensitive channels, only the channels reasonably insensitive to zinc as a blocker would exhibit augmentation of activity. KCNQ channels are indeed not very sensitive to such inhibition ([Fig. S4]).

Our hypothesis (Fig. 7) also can explain the highly variable efficacy of ZnPy observed in various studies. Thus, a dramatic 24-fold augmentation of KCNQ4 current (at saturating voltages) has been reported (16), whereas the effect on KCNQ2/3 channels in that study was much smaller (approximately twofold). In our hands the augmentation of KCNQ4, KCNQ2/3, and native M channels by ZnPy, by other zinc ionophores, and by intracellular zinc in whole-cell recordings was in the range of 1.5- to threefold (Figs. 1–3) (52). However, much stronger effects were observed when PIP$_2$ levels were depleted (Fig. 2 C–F) or when the PIP$_2$ affinity of the channels was reduced by mutagenesis (Fig. 5 and [Fig. S6]). Thus, it is expected that the efficacy of ZnPy in augmenting KCNQ channel activity in any particular experimental setting will depend strongly on the channel saturation with PIP$_2$.

Our findings confirm the discovery of ZnPy as a potent KCNQ channel opener (16); however, our study differs significantly from the original publication in the interpretation of the mechanism of ZnPy action. It was originally proposed that the effect is produced by the pyrithione moiety (in complex with zinc) binding to the channel's pore region from the extracellular side (16). Here we briefly discuss the differences between that study (16) and our investigation. (*i*) Xiong et al. (16) reported only marginal effects of other zinc ionophores, i.e., DEDTC, DIQ, and α-tocopherol, on KCNQ2 channels. Zinc ionophore activity of α-tocopherol is not well documented, but the lack of effect of DEDTC and DIQ is perplexing, because in our hands both ionophores (as well as three others) strongly augmented KCNQ currents (Fig. 1). We also show that all the ionophores tested produced strong intracellular zinc accumulation (Fig. 1); because no such measurements were performed in the study by Xiong et al., (16), we suggest that under their experimental conditions ZnPy was superior to other ionophores in loading cells with zinc. (*ii*) Dialysis of 10 µM ZnPy through the recording pipette did not significantly affect the amplitude of the KCNQ2 current, but extracellular ZnPy was still effective. Therefore it was suggested that ZnPy acts from the extracellular side. However, this experiment is hard to interpret, because it is not clear how much free intracellular zinc has been delivered in such a way. Our experiments demonstrated that the direct application of ZnCl$_2$ to the intracellular side of the excised patch (Fig. 2 C–F) or by dialysis through the whole-cell pipette (Fig. 3F) strongly potentiated both recombinant and native KCNQ channels. (*iii*) The effect of 20 µM NaPy on KCNQ2 current was marginal; it was proposed that KCNQ2 interacts with pyrithione with low affinity, but the affinity is increased when pyrithione is in complex with zinc (16). In our experiments NaPy produced a significant increase of KCNQ4 current but, importantly, also elevated intracellular zinc, although both effects were much less pronounced than with ZnPy. This difference may arise from the cells in the previous study having a lower store of intracellular zinc.

Zinc is increasingly recognized as a ubiquitous second messenger, perhaps comparable in this regard to calcium (53). Cytosolic free zinc levels at rest are too low to affect KCNQ channel activity (<1 nM) (12); these low levels likely explain the observation that, although TPEN reversed the augmentation of the KCNQ current by exogenous zinc, it rarely reduced the amplitude of KCNQ channels overexpressed in nonexcitable CHO cells to levels below the baseline. However, zinc can reach millimolar levels in the synaptic vesicles of neurons (13); another releasable pool of zinc is bound to intracellular proteins such as metallothioneins (15). Vesicular zinc is released during synaptic transmission and loads postsynaptic terminals through zinc-permeable channels (e.g., AMPA) (14). Zinc also can be released from cytosolic buffers in response to acidification (15), as observed in hypoxic conditions. In a recent study FluoZin3 zinc imaging revealed large intracellular zinc transients (comparable to the rises recorded in this study in response to zinc ionophores) in hippocampal pyramidal neurons in response to oxidative stress (14). Therefore it is conceivable that augmentation of KCNQ channel activity by postsynaptic zinc accumulation could constitute a strategy to survive excitotoxicity produced by ischemia or other conditions linked to overexcitability, such as epileptic seizures. A strong protective role of M channels has been demonstrated in ischemic brain injury and stroke (reviewed in ref. 2). Importantly, because zinc makes KCNQ channels virtually insensitive to G$_{q/11}$ receptor inhibition, postsynaptic zinc elevations could maintain M channel activity in the face of enhanced neurotransmitter release. Further research is required to test these intriguing hypotheses.

Methods

Cell Culture, Transfection, Mutagenesis. HEK 293 cells were cultured in DMEM, and CHO cells were cultured in DMEM:F12 (1:1), both supplemented with GlutaMAX I, 10% FBS, penicillin (50 U/mL), and streptomycin (100 µg/mL); all cell culture reagents were from Gibco. DRG neurons from 7-d-old Wistar rats were dissociated as previously described (29) and were cultured in DMEM supplemented as above on glass coverslips that were coated with poly-D-lysine and laminin for 2–5 d in a humidified incubator (37 °C, 5% CO$_2$). CHO or HEK293 cells were transfected using FuGENE HD (Promega) with the following cDNA (routinely subcloned into pcDNA3.1): human KCNQ4 (GeneBank accession no. AF105202) and its mutants; KCNQ2/3 concatemer (a kind gift from Snezana Maljevic, Tubingen University, Tubingen, Germany); KCNQ3 A315T and its mutants (kindly provided by Mark Shapiro, University of Texas Health Science Center at San Antonio, San Antonio, TX); type 1a PI(4)5-kinase (54); PLC-δPH-GFP (55); and ciVSP (40) (a kind gift from Tibor Rohacs, Rutgers New Jersey Medical School, Rutgers University, Newark, NJ). The point mutations and truncations were introduced by site-directed mutagenesis using standard techniques and were verified by sequencing. All experimental procedures on animals followed the guidelines and recommendations of the UK Home Office, were covered by a Home Office license (to N.G.), and were in accordance with the regulations of the UK Animals (Scientific Procedures) Act 1986.

Whole-Cell and Perforated-Patch Recordings. All recordings were made using an EPC10 amplifier in combination with PatchMaster v2 software and analyzed using the FitMaster v2 (all from HEKA Instruments). Most of the whole-cell recordings were made using perforated patch-clamp technique. The standard bath solution contained the following (in mM): 160 NaCl, 2.5 KCl, 1 MgCl$_2$, 2 CaCl$_2$, 10 Hepes (pH 7.4 with NaOH), 305–310 mOsm/kg. The standard pipette solution contained the following (in mM): 160 KCl, 5.0 MgCl$_2$, 5.0 Hepes, 0.1 BAPTA, 3 K$_2$ATP, NaGTP, (pH 7.4 with KOH), supplemented with amphotericin B (200–400 µg/mL). Unless stated otherwise, all reagents used in electrophysiology and imaging experiments were from Sigma-Aldrich. The access resistance was typically within 5 MΩ. For recordings from DRG neurons, small-diameter cells (~20 µm) were selected. For applying ZnCl$_2$ (50 µM) to the cytosol of DRG neurons via patch pipette dialysis, the conventional whole-cell configuration was used. The pipette solution contained the following (in mM): 120 K-acetate, 35 KCl, 5 NaCl, 3NaATP, 0.1 GTP, 10 Hepes (pH 7.3 with KOH). KCNQ/M currents were measured by a 1-s square voltage pulse to –60 mv from a holding potential of 0 mV (CHO cells) or –30 mV (DRG neurons) applied every 2 s. Recombinant KCNQ current amplitude was defined as XE991-sensitive steady-state outward current amplitude at 0 mV. Native M current amplitude was defined as XE991-sensitive tail current amplitude upon a voltage step from –30 to –60 mV. In experiments with ciVSP, cells were held at –80 mV and three-step voltage pulses (a 1-s step to –20 mV followed by a 1-s step to 120 mV and a 30-s step back to –20 mV) were applied with 3-s intervals.

Single-Channel Recording. The inside-out KCNQ current recording and analysis were performed as before (6, 8). Channel activity was recorded 48–72 h after transfection; pipettes had resistances of 7–15 MΩ when filled with a solution of the following composition (in mM): 150 NaCl, 5 KCl, 1 MgCl$_2$, and 10 Hepes (pH 7.4 with NaOH). The extracellular solution contained the following (in mM): 175 KCl, 4 MgCl$_2$, and 10 Hepes (pH 7.4 with KOH). The resting membrane voltage was assumed to be 0 mV. Currents were recorded using an EPC

10 amplifier (HEKA Instruments), sampled at 5 kHz, and filtered at 0.5–1 kHz. Single-channel data (including P_o histogram generation) were analyzed using FitMaster software (HEKA Instruments). Methods for event analysis and calculation of P_o and single-channel amplitude were as described in ref. 6.

Fluorescence Imaging. Intracellular zinc imaging was performed as described in ref. 19. CHO cells or DRG cultures were loaded with FluoZin-3 AM (Thermo Fisher) (5 μM for 30 min at 37 °C in the presence of 0.02% pluronic F-127). Cells were washed with an extracellular bath solution composed of the following (in mM): 160 NaCl, 2.5 KCl, 2 CaCl$_2$, 1 MgCl$_2$, and 10 Hepes (pH 7.4 with NaOH). Cells were imaged using a Leica SP5 fluorescence imaging system assembled on a Leica DMI6000 microscope and illuminated with 488-nm light for 1,200 ms (400 Hz) with a 2-s interval. In confocal PIP$_2$ imaging experiments, HEK293 cells transfected with PLC-δPH-GFP and KCNQ4 were illuminated using Nikon A1 confocal microscope with a 488-nm argon laser. Images were collected on an electron-multiplying CCD camera (DQC-FS; Nikon) using NIS Elements 4.0 imaging software (Nikon), which also was used for analysis.

Statistics. All data are given as mean ± SEM. Differences between groups were assessed by Student's t test (paired or unpaired, as appropriate) or one-way ANOVA with Bonferroni correction. The differences were considered significant at $P \leq 0.05$.

1. Delmas P, Brown DA (2005) Pathways modulating neural KCNQ/M (Kv7) potassium channels. *Nat Rev Neurosci* 6:850–862.
2. Gamper N, Shapiro MS (2015) KCNQ channels. *Handbook of Ion Channels*, eds Zheng J, Trudeau MC (CRC, Boca Raton, FL), 1st Ed, pp 275–306.
3. Gribkoff VK (2008) The therapeutic potential of neuronal Kv7 (KCNQ) channel modulators: An update. *Expert Opin Ther Targets* 12:565–581.
4. Suh BC, Hille B (2002) Recovery from muscarinic modulation of M current channels requires phosphatidylinositol 4,5-bisphosphate synthesis. *Neuron* 35:507–520.
5. Zhang H, et al. (2003) PIP$_2$ activates KCNQ channels, and its hydrolysis underlies receptor-mediated inhibition of M currents. *Neuron* 37:963–975.
6. Li Y, Gamper N, Hilgemann DW, Shapiro MS (2005) Regulation of Kv7 (KCNQ) K$^+$ channel open probability by phosphatidylinositol 4,5-bisphosphate. *J Neurosci* 25:9825–9835.
7. Telezhkin V, Brown DA, Gibb AJ (2012) Distinct subunit contributions to the activation of M-type potassium channels by PI(4,5)P$_2$. *J Gen Physiol* 140:41–53.
8. Li Y, Gamper N, Shapiro MS (2004) Single-channel analysis of KCNQ K$^+$ channels reveals the mechanism of augmentation by a cysteine-modifying reagent. *J Neurosci* 24:5079–5090.
9. Zaydman MA, Cui J (2014) PIP$_2$ regulation of KCNQ channels: Biophysical and molecular mechanisms for lipid modulation of voltage-dependent gating. *Front Physiol* 5:195.
10. Salzer I, et al. (2017) Phosphorylation regulates the sensitivity of voltage-gated Kv7.2 channels towards phosphatidylinositol-4,5-bisphosphate. *J Physiol* 595:759–776.
11. Kim HJ, et al. (2016) Protein arginine methylation facilitates KCNQ channel-PIP$_2$ interaction leading to seizure suppression. *Elife* 5:e17159.
12. Takeda A (2014) Zinc signal in brain functions. *Zinc Signals in Cellular Functions and Disorders*, eds Fukada T, Kambe T (Springer, Tokyo), pp 161–181.
13. Sindreu C, Storm DR (2011) Modulation of neuronal signal transduction and memory formation by synaptic zinc. *Front Behav Neurosci* 5:68.
14. Medvedeva YV, Ji SG, Yin HZ, Weiss JH (2017) Differential vulnerability of CA1 versus CA3 pyramidal neurons after ischemia: Possible relationship to sources of Zn^{2+} accumulation and its entry into and prolonged effects on mitochondria. *J Neurosci* 37:726–737.
15. Kiedrowski L (2014) Proton-dependent zinc release from intracellular ligands. *J Neurochem* 130:87–96.
16. Xiong Q, Sun H, Li M (2007) Zinc pyrithione-mediated activation of voltage-gated KCNQ potassium channels rescues epileptogenic mutants. *Nat Chem Biol* 3:287–296.
17. Zhou P, et al. (2013) Phosphatidylinositol 4,5-bisphosphate alters pharmacological selectivity for epilepsy-causing KCNQ potassium channels. *Proc Natl Acad Sci USA* 110:8726–8731.
18. Magda D, et al. (2008) Synthesis and anticancer properties of water-soluble zinc ionophores. *Cancer Res* 68:5318–5325.
19. Huang D, et al. (2016) Redox-dependent modulation of T-type Ca^{2+} channels in sensory neurons contributes to acute anti-nociceptive effect of substance P. *Antioxid Redox Signal* 25:233–251.
20. Kim CH, Kim JH, Xu J, Hsu CY, Ahn YS (1999) Pyrrolidine dithiocarbamate induces bovine cerebral endothelial cell death by increasing the intracellular zinc level. *J Neurochem* 72:1586–1592.
21. Kim CH, et al. (2000) Biphasic effects of dithiocarbamates on the activity of nuclear factor-kappaB. *Eur J Pharmacol* 392:133–136.
22. Kojima R, Kamata S (1994) Zinc-selective membrane electrode using tetrabutyl thiuram disulfide neutral carrier. *Anal Sci* 10:409–412.
23. Prachayasittikul V, Prachayasittikul S, Ruchirawat S, Prachayasittikul V (2013) 8-hydroxyquinolines: A review of their metal chelating properties and medicinal applications. *Drug Des Devel Ther* 7:1157–1178.
24. Gamper N, et al. (2006) Oxidative modification of M-type K$^+$ channels as a mechanism of cytoprotective neuronal silencing. *EMBO J* 25:4996–5004.
25. Canzoniero LM, Manzerra P, Sheline CT, Choi DW (2003) Membrane-permeant chelators can attenuate Zn^{2+}-induced cortical neuronal death. *Neuropharmacology* 45:420–428.
26. Crouch PJ, Barnham KJ (2012) Therapeutic redistribution of metal ions to treat Alzheimer's disease. *Acc Chem Res* 45:1604–1611.
27. Telezhkin V, Reilly JM, Thomas AM, Tinker A, Brown DA (2012) Structural requirements of membrane phospholipids for M-type potassium channel activation and binding. *J Biol Chem* 287:10001–10012.
28. Gamper N, Rohacs T (2012) Phosphoinositide sensitivity of ion channels, a functional perspective. *Subcell Biochem* 59:289–333.
29. Du X, et al. (2014) Control of somatic membrane potential in nociceptive neurons and its implications for peripheral nociceptive transmission. *Pain* 155:2306–2322.
30. Rose K, et al. (2011) Transcriptional repression of the M channel subunit Kv7.2 in chronic nerve injury. *Pain* 152:742–754.
31. Du X, Gamper N (2013) Potassium channels in peripheral pain pathways: Expression, function and therapeutic potential. *Curr Neuropharmacol* 11:621–640.
32. Ooi L, Gigout S, Pettinger L, Gamper N (2013) Triple cysteine module within M-type K$^+$ channels mediates reciprocal channel modulation by nitric oxide and reactive oxygen species. *J Neurosci* 33:6041–6046.
33. Krezel A, Hao Q, Maret W (2007) The zinc/thiolate redox biochemistry of metallothionein and the control of zinc ion fluctuations in cell signaling. *Arch Biochem Biophys* 463:188–200.
34. Vallee BL, Falchuk KH (1993) The biochemical basis of zinc physiology. *Physiol Rev* 73:79–118.
35. Gamper N, Li Y, Shapiro MS (2005) Structural requirements for differential sensitivity of KCNQ K$^+$ channels to modulation by Ca^{2+}/calmodulin. *Mol Biol Cell* 16:3538–3551.
36. Zaika O, Hernandez CC, Bal M, Tolstykh GP, Shapiro MS (2008) Determinants within the turret and pore-loop domains of KCNQ3 K$^+$ channels governing functional activity. *Biophys J* 95:5121–5137.
37. Hernandez CC, Falkenburger B, Shapiro MS (2009) Affinity for phosphatidylinositol 4,5-bisphosphate determines muscarinic agonist sensitivity of Kv7 K$^+$ channels. *J Gen Physiol* 134:437–448.
38. Hernandez CC, Zaika O, Shapiro MS (2008) A carboxy-terminal inter-helix linker as the site of phosphatidylinositol 4,5-bisphosphate action on Kv7 (M-type) K$^+$ channels. *J Gen Physiol* 132:361–381.
39. Telezhkin V, Thomas AM, Harmer SC, Tinker A, Brown DA (2013) A basic residue in the proximal C-terminus is necessary for efficient activation of the M-channel subunit Kv7.2 by PI(4,5)P$_2$. *Pflugers Arch* 465:945–953.
40. Iwasaki H, et al. (2008) A voltage-sensing phosphatase, Ci-VSP, which shares sequence identity with PTEN, dephosphorylates phosphatidylinositol 4,5-bisphosphate. *Proc Natl Acad Sci USA* 105:7970–7975.
41. Falkenburger BH, Jensen JB, Hille B (2010) Kinetics of PIP$_2$ metabolism and KCNQ2/3 channel regulation studied with a voltage-sensitive phosphatase in living cells. *J Gen Physiol* 135:99–114.
42. Kruse M, Hammond GR, Hille B (2012) Regulation of voltage-gated potassium channels by PI(4,5)P$_2$. *J Gen Physiol* 140:189–205.
43. Okamura Y, Murata Y, Iwasaki H (2009) Voltage-sensing phosphatase: Actions and potentials. *J Physiol* 587:513–520.
44. Stauffer TP, Ahn S, Meyer T (1998) Receptor-induced transient reduction in plasma membrane PtdIns(4,5)P$_2$ concentration monitored in living cells. *Curr Biol* 8:343–346.
45. Mavrantoni A, et al. (2015) A method to control phosphoinositides and to analyze PTEN function in living cells using voltage sensitive phosphatases. *Front Pharmacol* 6:68.
46. Wald T, et al. (2014) Quantification of potassium levels in cells treated with *Bordetella* adenylate cyclase toxin. *Anal Biochem* 450:57–62.
47. Zaydman MA, et al. (2013) Kv7.1 ion channels require a lipid to couple voltage sensing to pore opening. *Proc Natl Acad Sci USA* 110:13180–13185.
48. Zhang Q, et al. (2013) Dynamic PIP$_2$ interactions with voltage sensor elements contribute to KCNQ2 channel gating. *Proc Natl Acad Sci USA* 110:20093–20098.
49. Park KH, et al. (2005) Impaired KCNQ1-KCNE1 and phosphatidylinositol-4,5-bisphosphate interaction underlies the long QT syndrome. *Circ Res* 96:730–739.
50. Suh BC, Hille B (2007) Electrostatic interaction of internal Mg^{2+} with membrane PIP$_2$ seen with KCNQ K$^+$ channels. *J Gen Physiol* 130:241–256.
51. Du X, et al. (2004) Characteristic interactions with phosphatidylinositol 4,5-bisphosphate determine regulation of kir channels by diverse modulators. *J Biol Chem* 279:37271–37281.
52. Linley JE, Pettinger L, Huang D, Gamper N (2012) M channel enhancers and physiological M channel block. *J Physiol* 590:793–807.
53. Fukada T, Yamasaki S, Nishida K, Murakami M, Hirano T (2011) Zinc homeostasis and signaling in health and diseases: Zinc signaling. *J Biol Inorg Chem* 16:1123–1134.
54. Bender K, Wellner-Kienitz MC, Pott L (2002) Transfection of a phosphatidyl-4-phosphate 5-kinase gene into rat atrial myocytes removes inhibition of GIRK current by endothelin and alpha-adrenergic agonists. *FEBS Lett* 529:356–360.
55. Liu B, et al. (2010) The acute nociceptive signals induced by bradykinin in rat sensory neurons are mediated by inhibition of M-type K$^+$ channels and activation of Ca^{2+}-activated Cl$^-$ channels. *J Clin Invest* 120:1240–1252.

NEUROSCIENCE